



RESEARCH ARTICLE



A surface network based method for studying urban hierarchies by night time light remote sensing data

Bin Wu^{a,b}, Bailang Yu ^{a,b}, Shenjun Yao^{a,b}, Qiusheng Wu ^c, Zuoqi Chen^{a,b}
and Jianping Wu^{a,b}

^aKey Laboratory of Geographic Information Science (Ministry of Education), East China Normal University, Shanghai, China; ^bSchool of Geographic Sciences, East China Normal University, Shanghai, China;

^cDepartment of Geography, Binghamton University, State University of New York, Binghamton, NY, USA

ABSTRACT

Urban hierarchies are closely related to economic growth, urban planning and sustainable urban development. Due to the limited availability of reliable statistical data at fine scales, most existing studies on urban hierarchy characterization failed to capture the detailed urban spatial structure information. Previous studies have demonstrated that night time light data are correlated with many urban socio-economic indicators and hence can be used to characterize urban hierarchies. This paper presents a novel method for studying urban hierarchies from night time light data. Night time light data were first conceptualized as continuous mathematical surfaces, termed *night time light surfaces*. From the morphology of these surfaces the corresponding surface networks were derived. Hereafter, a *night time light intensity (NTLI) graph* was defined to describe the morphology of the surface network. Then, structural similarity between the night time light surfaces of any two different cities was calculated via a threshold-based *maximum common induced graph* searching algorithm. Finally, urban hierarchies were defined on the basis of the structural similarities between different cities. Using the 2015 annual NPP-VIIRS night time light data, the urban hierarchies of 32 major cities in China were successfully examined. The results are highly consistent with the reference urban hierarchies.

ARTICLE HISTORY

Received 14 May 2018

Accepted 18 February 2019

KEYWORDS

Structural similarity; surface networks; urban hierarchy; night time light; graph theory

Introduction

An *urban hierarchy* is defined as the general organization of various scales and types of cities within a region (Pumain 2006). It exerts a strong influence on new town planning and construction, urban agglomeration and spatial development strategies in the context of regional cooperation (Okabe and Masuda 1984, Sadahiro 2001, Okabe and Masuyama 2006, Masuda 2009). Due to the economic, environmental and social implications of urbanization, the structures of urban hierarchical systems were always in the focus of national and local governments. Governments and urban planners use the concept of urban hierarchies to study the location of public facilities, to promote urban

agglomeration effects and to make comprehensive planning decisions (Joao *et al.* 2014). Constructing a scientific and reasonable urban hierarchy system is not only an effective way to improve social and economic management mechanisms (Bettencourt 2013), but also the key to understanding the similarities and differences of urbanizing cities.

Research on urban hierarchies can be traced back to the well-known *Central Place Theory*, which explains the spatial arrangement of settlements and goes back to the German geographer Christaller (1933). In the years to follow, a wide range of models and analytical methods were developed for measuring urban hierarchies, such as the urban primacy ratio (Rosen and Resnick 1980), the fractal dimension (Batty *et al.* 1989), *Zipf's Law for Cities* (Newman 2005) or *Gibrat's Law for (All) Cities* (Eeckhout 2004). In traditional studies, urban hierarchies were characterized by a rank/size distribution demographically or a more systematic classification schemes functionally (Beaverstock *et al.* 1999, Guerrero and Proulhac 2014). In the first approach, demographic parameters were used as an approximation for the centrality of cities' markets (Neal 2011), defining urban hierarchies in terms of population size (Borchert 1967, Lorenzen and Andersen 2009, Maliszewski and Huallacháin 2012) or employment rates (Partridge *et al.* 2008). In the second approach, functional criteria were applied, such as, for example, the prevalence of global firms (Beaverstock *et al.* 1999), airline passenger information (Taaffe 1962, Xue 2008, Neal 2011), Gross Domestic Product (GDP) (Fang and Yu 2017), freight flows (Zhong and Lu 2011, Guerrero and Proulhac 2014) or housing costs (Partridge *et al.* 2009). Other studies investigated urban hierarchies by examining differences and similarities between demographical distributions within cities. For example, Okabe and Masuda (1984) used a quadratic function to approximate urban hierarchies from two-dimensional population distributions. Okabe and Masuyama (2006) proposed a quantitative approach based on the structural similarity of population distributions in Japan cities to classify urban hierarchies.

Although the previously described approaches, which focused on the hierarchical structure and distribution pattern of urban systems, are straightforward and work well in a statistical context, they suffer from some drawbacks. First of all, in several approaches only one of the available census variables was used, such as, the total population, GDP or employment rate. However, no single variable can measure the actual population size/distribution in an urban space (Mu and Wang 2006, Zhong *et al.* 2017). Secondly, more recent studies focused on factors responsible for structuring urban hierarchies, thereby neglecting the important role of urban spatial structure (Chen 1991, Bretagnolle *et al.* 2009, Chen and Wang 2014, Fang *et al.* 2017). As the features being investigated in previous studies were of low resolution, urban structures and zoning information could obviously not be captured adequately. Thirdly, previous approaches suffered from the unreliability and unavailability of statistical data (Wu *et al.* 2014). Thus, new objective data sources and quantitative methods for examining urban hierarchies are urgently needed.

Recently developed remote sensing technologies offer new opportunities for studying urban hierarchies, as they can provide information about urban regions at a high resolution and for large areas. Among these data, night time light data have become

a research hotspot as they provide the means to overcome the scarcity of global urban information (Mellander *et al.* 2015). Night time light data record the light emission from Earth's surface at night, thus reflecting the intensity of human activities (Elvidge *et al.* 1997). Researchers found that night time light data can visualize different social and economic aspects of cities, such as urban areas' delineations (Small *et al.* 2005, Yu *et al.* 2014), carbon dioxide emissions (Shi *et al.* 2016a), total freight traffic mappings (Shi *et al.* 2015), gross domestic products' estimations (Shi *et al.* 2014), economic activities' measurements (Mellander *et al.* 2015), electric power consumptions (Shi *et al.* 2016b), poverty evaluations (Yu *et al.* 2015) and violent conflict analysis (Li and Li 2014, Li *et al.* 2015). More importantly, night time light data also help urban researchers to gain new insights in urban structures (Welch 1980, Liu *et al.* 2012, Small *et al.* 2013, Yu *et al.* 2014, Chen *et al.* 2017) and urban hierarchies (Wu *et al.* 2014, Zhang *et al.* 2015). Regarding the remarkable correlation between night time light data and urban features, night time light data can serve as an objective data source to provide unprecedented possibilities for studying the differences or similarities of urban hierarchies among different cities (Wu *et al.* 2014, Zhang *et al.* 2015). However, until today little research based on night time light data has been conducted on the hierarchical structures and distribution patterns of urban systems.

The present study has two objectives, namely, (1) to investigate the feasibility of applying night time light data to examine urban hierarchies and (2) to introduce a novel method for studying urban hierarchies by night time light data. Inspired by the method of Okabe and Masuyama (2006), our approach examines urban hierarchies by measuring the structural similarity of night time light data between different cities. First of all, night time light data were conceptualized as continuous mathematical surfaces, termed *night time light surfaces*. From the morphology of these surfaces the corresponding surface networks were derived. Hereafter, a *night time light intensity (NTLI) graph* was defined to describe the morphology of the surface. In a next step, the structural similarity between the night time light surfaces of any two different cities was calculated via a threshold-based *maximum common induced graph* searching algorithm. Finally, urban hierarchies were defined on the basis of the structural similarities between different cities. The remainder of this paper is organized as follows. In Section 2 the study area and the data used within this study are described, while in Section 3 the methodological framework is presented. In Section 4 the obtained results are presented, whereas in Section 5 the applicability of the approach including its limitations is discussed. In Section 6, finally, conclusions with respect to future research and applications are drawn.

Study area and data

Study area

In this study, 32 major cities in China with different levels of urbanization and socio-economic development were selected as study areas. All of them are municipalities or provincial capitals, with the exception of Shenzhen, which was established as a *special economic zone* in 1978 and is now considered as a major financial center in southern China. These cities were grouped into six regions according to the geography of China (Fang *et al.* 2001): North, Northeast, East, Central-south, Southwest and Northwest.

Beijing (BJ), Tianjin (TJ), Hohhot (HT), Taiyuan (TY) and Shijiazhuang (SJZ) are situated in the North China region; Harbin (HB), Changchun (CC) and Shenyang (SY) lie in the Northeast; Urumqi (UQ), Xining (XN), Lanzhou (LZ), Xi'an (XA) and Yinchuan (YC) are seated in the Northwest; Shanghai (SH), Nanjing (NJ), Hangzhou (HZ), Hefei (HF), Jinan (JN), Nanchang (NC) and Fuzhou (FZ) are located in the East; Wuhan (WH), Zhengzhou (ZZ), Changsha (CS), Guangzhou (GZ), Shenzhen (SZ), Nanning (NN) and Haikou (HK) are part of the Central-south; Chengdu (CD), Chongqing (CQ), Guiyang (GY), Kunming (KM) and Lhasa (LS), finally, lie in the Southwest. Most highly urbanized cities are located in the East, Northeast, Central-south and North regions, while the cities with moderate and lower urbanization levels are found in the Southwest and Northwest regions.

Data

In early 2013, the National Oceanic and Atmospheric Administration's National Geophysical Data Center (NOAA/NGDC) released a new generation of night time light data, which were derived from a sensor named *Visible Infrared Imaging Radiometer Suite (VIIRS)* onboard the *Suomi National Polar-Orbiting Partnership (Suomi NPP)*. In this study, the version 1 annual NPP-VIIRS night time light composite data of 2015 (https://www.ngdc.noaa.gov/eog/viirs/download_dnb_composites.html, accessed March 2018) were used. The released NPP-VIIRS night time light composite data were filtered to exclude data affected by stray light, lunar illumination and cloud-cover. The NPP-VIIRS night time light composite data contain floating point radiance values with units in $\text{nano-Wcm}^{-2}\text{sr}^{-1}$. The annual NPP-VIIRS night time light composite data for 2015 were converted to the Albers Equal Area Conic projection with a pixel size of 500 m. The data were corrected to remove background noise and outliers by using the method proposed by Shi *et al.* (2014). For each city, the night time light data were extracted from the annual NPP-VIIRS night time light composite data by using the mask polygon of the city's administrative boundary.

Methodology

Theoretical basis of surface networks

As mentioned earlier, night time light intensity reflects the human activities' intensity on Earth's surface, whereby a higher value of night time light intensity represents a higher concentration of human activities. As a consequence, the night time light data for a region can be conceptualized as a continuous surface $Z = f(x, y)$ (see Figure 1(a)) (Chen *et al.* 2017), which is termed *night time light surface*. A three-dimensional view of a night time light surface is depicted in Figure 1(c).

With respect to the formal characterization of *critical points*, two assumptions concerning the function $Z = f(x, y)$ have to be made (Pfaltz 1976, Wolf 1991, 2004, 2014, 2017). The first assumption is that $Z = f(x, y)$ is a *smooth function*, which means that it is differentiable for any number of times. The second assumption is that the function $Z = f(x, y)$ has only non-degenerate critical points, i.e. the well-known peaks, pits and passes (see Figure 1(b)). A critical point (x_0, y_0) can be characterized by $f_x(x_0, y_0) = f_y(x_0, y_0) = 0$, which means that the first-order partial derivatives at the point (x_0, y_0) vanish. The type

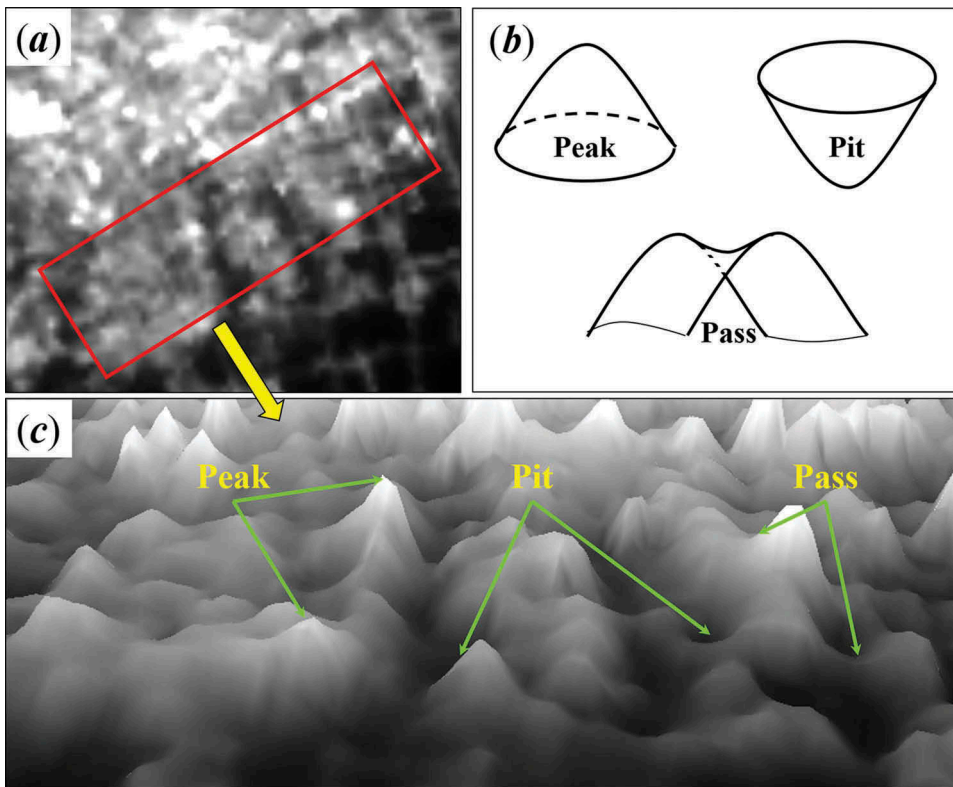


Figure 1. Night time light surfaces and critical points: (a) Two-dimensional view of a night time light surface; (b) three different types of critical points, namely, peak, pit and pass; (c) three-dimensional view of a section of the night time light surface shown in (a).

of the critical point can be achieved by examining the number of negative eigenvalues of the Hessian matrix $H_f(x_0, y_0) = \begin{pmatrix} f_{xx}(x_0, y_0) & f_{xy}(x_0, y_0) \\ f_{yx}(x_0, y_0) & f_{yy}(x_0, y_0) \end{pmatrix}$ at the critical point, whereby f_{xx} , f_{xy} , f_{yx} , and f_{yy} are the second-order partial derivatives of the function $f(x, y)$. If the number of negative eigenvalues of $H_f(x_0, y_0)$ is two, then $f(x, y)$ has a peak at (x_0, y_0) ; if the number of negative eigenvalues of $H_f(x_0, y_0)$ is one, then $f(x, y)$ has a pass at (x_0, y_0) ; if the number of negative eigenvalues of $H_f(x_0, y_0)$ is zero, then $f(x, y)$ has a pit at (x_0, y_0) (Wolf 2014). For these critical points the *Euler-Poincare formula*, which says that *the number of peaks – the number of passes + the number of pits = 2*, must hold, whereby the virtual pit (peak) has to be taken into account (Takahashi *et al.* 1995, Wolf 2014). In Figure 2(a), which visualizes a night time light surface, peaks, pits and passes are indicated by red triangles, blue triangles and yellow squares, respectively. With regard to night time light surfaces, peaks are regarded as concentration areas (such as urban centers), while pits are considered as sparse areas (such as urban villages) and passes are regarded as transition areas of human activities, respectively.

Of special interest with respect to surface analysis are also the lines connecting the peaks and passes, which are termed *ridge lines*, and the lines connecting the passes and pits, which are termed *course lines*. Both ridge lines and course lines are special cases of *integral lines*, i.e.

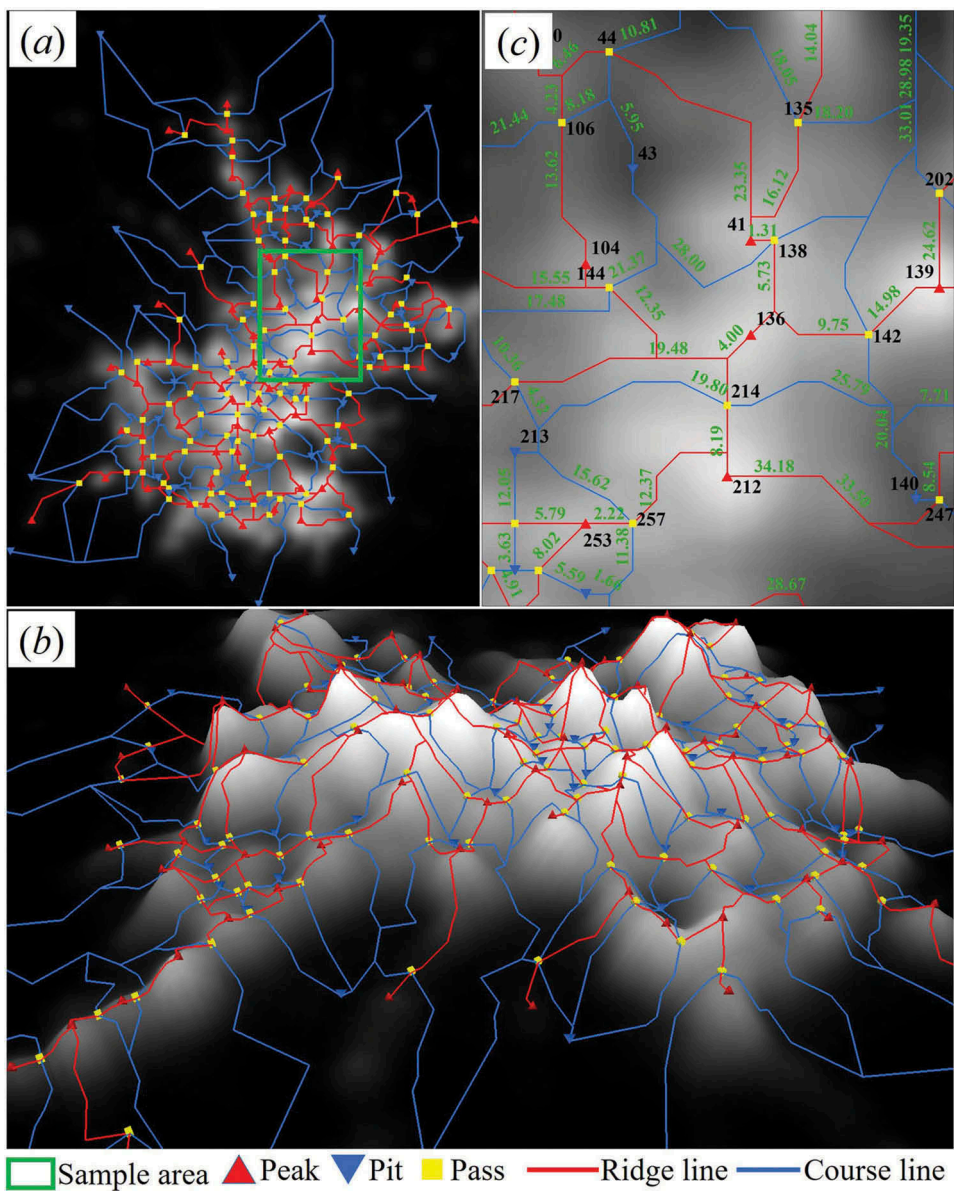


Figure 2. Night time light surface together with its associated NTLI graph: (a) two-dimensional view; (b) three-dimensional view; (c) NTLI graph of the surface located in the green box shown in (a).

they are lines that are maximal paths on a two-dimensional smooth compact manifold $f(x, y)$, which are everywhere tangent to the gradient vector field $\begin{pmatrix} f_x \\ f_y \end{pmatrix}$ (Wolf 2014). In Figure 2(a) ridge lines and course lines are indicated by red and blue lines, respectively.

The five critical features (i.e. peaks, pits, passes, ridge lines and course lines) define the surface network associated with the surface. Figure 2 visualizes the urban night time light surface with its corresponding surface network, whereby Figure 2(a,b) show a two-dimensional

three-dimensional view of the surface, respectively. For the sake of completeness, it should be noted that the critical points and critical lines were extracted from the night time light surface in a two-step process. First, a 3×3 mean filter was applied to smooth the surface, then the algorithm of Takahashi *et al.* (1995) was employed to extract the surface network from the corresponding smoothed night time light surface.

Night time light intensity graph

As graphs are mathematical structures eligible for representing both spatial and relational properties (Wu *et al.* 2015, 2017, 2018), the present study applies weighted surface networks for characterizing the topological structure of night time light surfaces. Weighted surface networks are edge-weighted and vertex-weighted graphs, with the weights indicating the importance of the respective features for the macro-structure and micro-structure of the corresponding surface. A formal definition of weighted surface networks can be found in Wolf (1991), Wolf (2004), Wolf (2014), Wolf (2017). Throughout the remainder of this paper, weighted surface networks representing the topology of night time light surfaces are termed *night time light intensity (NTLI) graphs*.

An NTLI graph G is an ordered pair of sets (V, E) , consisting of a nonempty set V of *vertices* together with a set E of *edges*, disjoint from V , whereby a pair of vertices is associated with each edge. To be precise, the vertices of an NTLI graph correspond to the critical points, while the edges correspond to the critical lines connecting the critical points. The NTLI graph of a night time light surface S is denoted by $G(S)$. In an NTLI graph G , each vertex v_i is weighted by its night time light intensity $I(v_i)$, while each edge $e(v_i, v_j)$ is weighted by the absolute difference of the night time light intensities of the two adjacent vertices v_i and v_j , i.e. $w(e(v_i, v_j)) = \text{abs}(I(v_i) - I(v_j))$. Figure 2(c) marks the vertex ID and edge weights of the ridges and courses for the NTLI graph, which corresponds to the surface network located in the green box shown in Figure 2(a).

Definition of structural similarity

Before introducing the concept of *structural similarity* formally, let us consider the two night time light surfaces S_1 and S_2 shown in Figure 3(a,b). When comparing the two surfaces, one can recognize that (a) the structures of the corresponding NTLI graphs $G(S_1)$ and $G(S_2)$ are similar, and (b) the night time light intensities $I(v_i)$ of the corresponding critical points are so close to each other that their differences are negligible. As a consequence, the two NTLI graphs $G(S_1)$ and $G(S_2)$ can be regarded as *structurally similar*, which means that they are *isomorphic* and *equally-weighted*. By definition, two graphs are regarded as isomorphic, if there exists a one-to-one correspondence between their vertices and edges. Specifically, let $G(S_1)$ and $G(S_2)$ denote two NTLI graphs of two night time light surfaces S_1 and S_2 , respectively. $e(v_i^1, v_j^1)$ and $e(v_m^2, v_n^2)$ denote two edges of $G(S_1)$ and $G(S_2)$, respectively. $e(v_i^1, v_j^1)$ is isomorphic to $e(v_m^2, v_n^2)$ if they satisfy

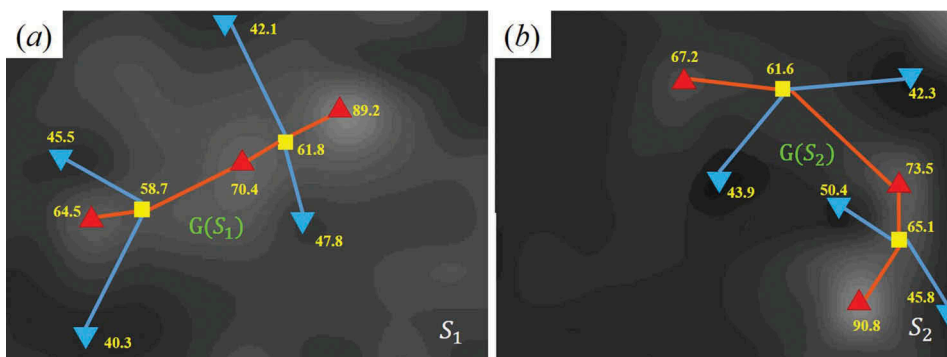


Figure 3. Comparison of two portions of night time light surfaces with their corresponding NTLI graphs: (a) NTL surface S_1 and its corresponding NTLI graph; (b) NTL surface S_2 and its corresponding NTLI graph.

the following equation: $I(v_i^1) = I(v_m^2)$ and $I(v_j^1) = I(v_n^2)$. On the contrary, $e(v_i^1, v_j^1)$ is not isomorphic to $e(v_m^2, v_n^2)$ if they do not satisfy the equation.

In graph theory, the determination of similarity between different graphs is often referred to as *inexact graph matching* (Raymond *et al.* 2002). Inexact graph matching is a process aiming to find the best possible matching between two different graphs. The most frequently used approach is to find the *maximum common induced subgraph* (MCIS) between the graphs being compared (Raymond *et al.* 2002, Raymond and Willett 2002). To better understand MCIS, some basic concepts have to be first introduced. A *subgraph* of a graph $G(S_i)$ is a graph, whose vertex set and edge set are subsets of $G(S_i)$. An *induced subgraph* is a set V of vertices of a graph $G(S_i)$ and those edges of $G(S_i)$ with both vertices in V . A graph $G(S_{ij})$ is a *common induced subgraph* of graphs $G(S_i)$ and $G(S_j)$ if $G(S_{ij})$ is isomorphic to induced subgraphs of $G(S_i)$ and $G(S_j)$. A *maximum common induced subgraph* consists of a graph $G(S_{ij})$ with the largest number of vertices meeting the property aforementioned. While MCIS, which are defined for unweighted graphs, can be determined by finding the corresponding vertices and edges from two graphs, in NTLIs both vertices and edges are weighted by real numbers, thus implying that an exact match between NTLI graphs can rarely be found. In this study, an MCIS algorithm that matches similar vertices and edges from two different NTLI graphs by applying a threshold-based matching method is proposed. To be precise, if the difference between the weights of two vertices from two different graphs is smaller than a pre-specified threshold w , i.e. $abs(I(v_i^1) - I(v_m^2)) < w$ and $abs(I(v_j^1) - I(v_n^2)) < w$, there is a one-to-one correspondence between these two vertices. As shown in Figure 4, the graph highlighted in bold is the maximum common induced subgraph of $G(S_1)$ and $G(S_2)$ by using a threshold $w = 5$.

Based on the threshold-based algorithm, all the possible matched vertices and edges between two NTLI graphs can be found. The next step is to find the MCIS between two different NTLI graphs by adapting an exhaustive search approach. It searches all the common subgraphs in an iterative manner, whereby the MCIS can be found. The algorithm description and pseudo-codes for the key technical components of our MCIS searching method can be found in supplementary material A. The MCIS searching is known as an NP-complete problem (Raymond *et al.* 2002, Chen *et al.* 2015). It means that the worst case time complexity is

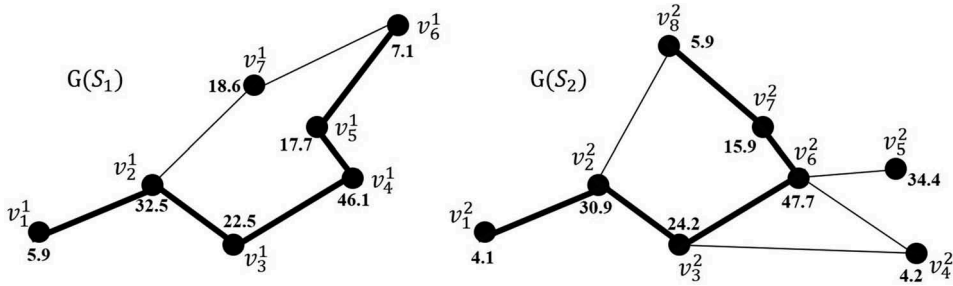


Figure 4. Maximum common induced subgraph (depicted in bold) of the two graphs $G(S_1)$ and $G(S_2)$.

exponential with respect to the number of nodes in the graphs. With an increasing number of vertices and edges of the input graphs, the requirements on computing power and computer memory can stack up rapidly. However, our MCIS search method has been adopted to avoid full iterations in two ways. First, the `PickNodeFromG2(u)` function in supplementary material A provides a highly ordered dataset containing one-to-one or one-to-many mappings among the vertices from two different graphs. These pre-ordered mappings can be retrieved directly. Second, only the vertices with mapping relationships are chosen for the iterations. Because the MCIS consists of the common vertices from two graphs, the vertices with no mapping relationships can be omitted directly from the `SearchMCIS()` function. This strategy also helps to minimize the need for computing power and computer memory.

Structural similarity index

In Section 3.3 the concept of the MCIS was introduced to define the structural similarity between two different NTLI graphs. To quantify the structural similarity between two NTLI graphs, a graph similarity index is introduced (Raymond *et al.* 2002). Let G_{12} denote the maximum common subgraph of two NTLI graphs G_1 and G_2 . $|V(G_1)|$, $|V(G_2)|$, and $|V(G_{12})|$ represent the number of vertices in G_1 , G_2 , and G_{12} , respectively. Similarly, $|E(G_1)|$, $|E(G_2)|$, and $|E(G_{12})|$ represent the number of edges in G_1 , G_2 , and G_{12} , respectively. Thus, the similarity index *sim* between G_1 and G_2 can be defined as follows:

$$\text{sim}(G_1, G_2) = \frac{(|V(G_{12})| + |E(G_{12})|)^2}{(|V(G_1)| + |E(G_1)|) \cdot (|V(G_2)| + |E(G_2)|)} \quad (1)$$

The similarity index $\text{sim}(G_1, G_2)$ ranges from 0 to 1. When two NTLI graphs G_1 and G_2 are completely isomorphic, $\text{sim}(G_1, G_2) = 1$; when two NTLI graphs G_1 and G_2 are not structurally similar at all, $\text{sim}(G_1, G_2) = 0$. The similarity index of $G(S_1)$ and $G(S_2)$ shown in Figure 4 was calculated to be 0.508.

Results

Urban hierarchies extracted from night time light data

After establishing the methodology for comparing night time light surfaces with respect to structural similarity, the technique was applied to 32 major cities in China. First, the

surface networks (Figure 5 and Figure S1 in supplementary material B) for the 32 cities were constructed from the 2015 annual NPP-VIIRS night time light data. As the 32 cities have different shapes and sizes of their administrative boundaries and also different urbanization levels, the distribution of night time light intensities differs between them. From Figure 5 and Figure S1 it can be seen, how the extracted surface networks vary in size and structure. In some cities, such as Changsha, Hangzhou, Lhasa, Nanchang or Xi'an, the corresponding surface networks are concentrated in the downtown areas, whereas in highly developed cities, such as Shanghai, Beijing, Tianjin or Shenzhen, the corresponding surface networks cover the entire city. The surface networks visualize the topological structure of the night time light data, providing not only an insight into the morphometry and spatial distribution of night time light but also an approximation of the urban spatial structure.

As can be seen from Figure 5, the number of peaks constituting the surface networks varies considerably. We summarized the number of the night time light peaks for each city by region in Figure 6. Obviously, the four directly controlled municipalities Shanghai, Beijing, Tianjin and Chongqing have the largest number of night time light peaks, whereas Xining, Haikou, Nanchang and Lhasa have the smallest ones. Because the night time light peaks are associated with the regions with a high density of human activities, the number of night time light peaks partly reflects the population distribution in combination with the level of economic development. Shanghai, Beijing, Tianjin and Chongqing, the four municipalities of China regarded as vanguards and engines of China's economic growth, have the highest number of night time light peaks, while

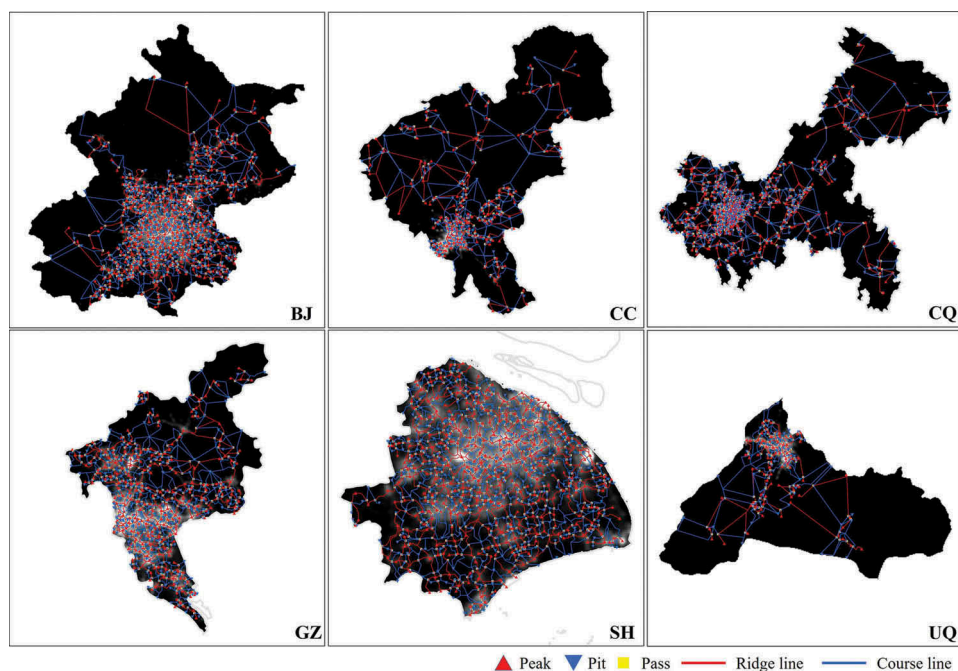


Figure 5. Surface networks corresponding to the night time light surfaces of six cities in China. Surface networks of the remaining 26 cities can be found in the supplementary material B.

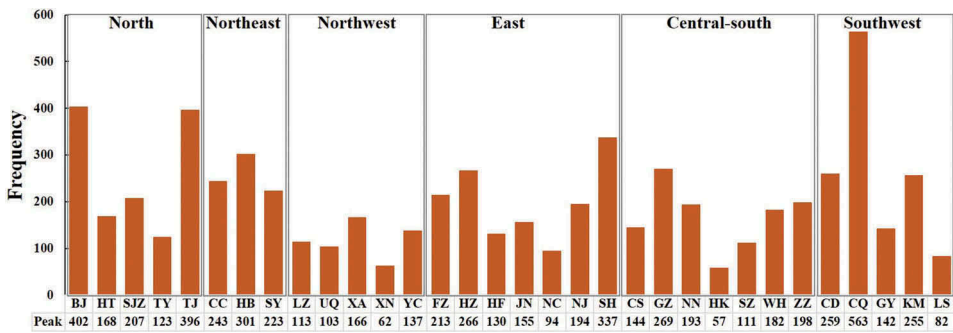


Figure 6. The number of peaks for 32 major Chinese cities.

many economically challenged cities in western and central China, such as Xining, Lhasa and Nanchang, have the lowest number of night time light peaks.

Based on the extracted night time light surface networks, the NTLI graphs for the 32 cities according to the method described in Section 3.2 were generated. Equation (1) was applied to calculate the structural similarity indices for all pairs of cities (resulting in a total of 496 combinations) by applying a threshold of $w = 5 \text{ nano-Wcm}^{-2}\text{sr}^{-1}$. All computations were conducted on a consumer-level PC with an Intel® Core i7, 3.0 GHz CPU, 16 GB RAM, running Windows® 7, 64-bit operating system. The total time for generating the surface networks was 1,984 seconds, while the time for calculating the 496 structural similarity indices was 579 minutes (the average elapsed time for each pair was approximately 3.2 minutes).

The matrix containing the similarity indices between the 32 cities is shown in Table 1. As can be seen in Table 1, the highest night time light surface similarity index (0.9321) is between Hangzhou and Guangzhou, while the lowest similarity index (0.0457) is between Lhasa and Chongqing. The distribution of the 496 structural similarity indices is shown in Figure 7. As can be seen from Figure 7, 60% of the structural similarity indices are less than 0.5, while only 4% of the structural similarity indices are larger than 0.8. The result indicates that the spatial structures of these 32 cities are quite different. The larger the difference between the night time light distributions of the two cities is, the smaller the respective structural similarity index will be.

To provide a visual representation of the structural similarity among the 32 cities, the *multidimensional scaling* (MDS) method was applied to map the pattern of structural similarities. MDS is an exploratory data analysis technique that provides a visual representation of dissimilarities (or similarities) between a set of objects. In other words, the technique attempts to find the hidden structures in data by rescaling a set of dissimilarities measurements into distances assigned to specific locations in a spatial configuration (Tsogo *et al.* 2000). Objects that are similar to each other lie close together, while dissimilar objects are further apart. Starting with the structural similarity indices given in Table 1, the 32 major cities of China were clustered by the MDS method described above and implemented in MATLAB®. The result of the clustering process is shown in Figure 8.

As shown in Figure 8, the 32 cities can be clustered into four groups. The first group (G1), located in the upper-left of the MDS map, comprises four cities, namely, Shanghai, Beijing, Chongqing and Tianjin. The second group (G2) covers five cities,

Table 1. Structural similarity indices between the 32 major cities of China.

	BJ	CC	CS	CD	CQ	FZ	GZ	GY	HK	HZ	HB	HF	HT	JN	KM	LZ
BJ	1.0000	—	—	—	—	—	—	—	—	—	—	—	—	—	—	—
CC	0.3893	1.0000	—	—	—	—	—	—	—	—	—	—	—	—	—	—
CS	0.2782	0.5341	1.0000	—	—	—	—	—	—	—	—	—	—	—	—	—
CD	0.5288	0.6375	0.3337	1.0000	—	—	—	—	—	—	—	—	—	—	—	—
CQ	0.6532	0.2227	0.1436	0.3456	1.0000	—	—	—	—	—	—	—	—	—	—	—
FZ	0.3379	0.6648	0.6406	0.5738	0.2416	1.0000	—	—	—	—	—	—	—	—	—	—
GZ	0.5998	0.4985	0.3163	0.7879	0.4253	0.5343	1.0000	—	—	—	—	—	—	—	—	—
GY	0.3100	0.6056	0.8447	0.4132	0.2283	0.5284	0.9321	1.0000	—	—	—	—	—	—	—	—
HK	0.0956	0.1844	0.2299	0.1555	0.0714	0.2087	0.1565	0.2724	1.0000	—	—	—	—	—	—	—
HZ	0.5759	0.4799	0.3037	0.7611	0.4288	0.5284	0.9321	0.3727	0.1358	1.0000	—	—	—	—	—	—
HB	0.5335	0.6225	0.4246	0.8131	0.3802	0.5252	0.8166	0.4815	0.1600	0.4081	1.0000	—	—	—	—	—
HF	0.2760	0.5330	0.6611	0.4670	0.1882	0.6228	0.4421	0.7814	0.3033	0.4081	0.4226	1.0000	—	—	—	—
HT	0.3036	0.6026	0.5229	0.5097	0.2151	0.6711	0.4711	0.8611	0.0994	0.4093	0.4780	0.7230	1.0000	—	—	—
JN	0.3292	0.6379	0.5505	0.5649	0.2491	0.7732	0.5297	0.6692	0.2439	0.5401	0.5071	0.6862	0.7664	1.0000	—	—
KM	0.5077	0.5549	0.3312	0.8558	0.3619	0.5681	0.8262	0.5379	0.1638	0.7519	0.7728	0.4770	0.5190	0.5709	1.0000	—
LZ	0.2029	0.3999	0.2660	0.1286	0.1216	0.4676	0.3416	0.6471	0.3714	0.1129	0.3317	0.2547	0.5394	0.2078	0.3630	1.0000
LS	0.0553	0.1170	0.1518	0.0861	0.0457	0.1408	0.0830	0.1728	0.0637	0.0813	0.0951	0.1909	0.1500	0.1534	0.0963	0.2525
NC	0.1995	0.3819	0.2703	0.3423	0.1491	0.4630	0.3194	0.6137	0.0770	0.3234	0.3036	0.6966	0.5457	0.5807	0.3418	0.2898
NJ	0.1952	0.6816	0.6396	0.3268	0.2061	0.7814	0.5437	0.7253	0.2258	0.2960	0.5386	0.6384	0.6912	0.5361	0.4855	0.4927
NN	0.3228	0.6529	0.6904	0.5453	0.2344	0.7828	0.5032	0.7751	0.2383	0.4657	0.5201	0.6833	0.7515	0.8207	0.5780	0.5318
SH	0.8174	0.4379	0.2237	0.5836	0.4795	0.3927	0.6910	0.3606	0.1125	0.6635	0.6314	0.3182	0.3495	0.3808	0.5957	0.2473
SY	0.4333	0.8638	0.5403	0.6964	0.3072	0.6698	0.6374	0.6051	0.1949	0.5436	0.6652	0.5347	0.6068	0.6453	0.6930	0.4220
SZ	0.1873	0.3656	0.4867	0.3103	0.1094	0.4115	0.2965	0.3857	0.4075	0.2694	0.2818	0.6122	0.4231	0.4858	0.3148	0.2570
SJZ	0.4477	0.6417	0.5847	0.7536	0.3324	0.6898	0.7107	0.6401	0.1866	0.7057	0.6815	0.5622	0.6018	0.7020	0.7672	0.4464
TY	0.2296	0.4629	0.2371	0.1780	0.0595	0.1879	0.1413	0.2504	0.3580	0.1241	0.1459	0.2828	0.5608	0.2229	0.1552	0.3399
TJ	0.8571	0.5025	0.3097	0.5973	0.5826	0.3847	0.6774	0.3512	0.1150	0.6394	0.6004	0.3082	0.3511	0.3699	0.5787	0.2419
UQ	0.1821	0.3434	0.2254	0.2835	0.0569	0.1829	0.1321	0.2341	0.4183	0.1277	0.2921	0.2678	0.4963	0.2241	0.2922	0.3161
WH	0.3728	0.7309	0.6271	0.6135	0.2804	0.7625	0.5970	0.7168	0.2365	0.5530	0.5845	0.6308	0.6914	0.7549	0.6301	0.4834
XA	0.1761	0.6391	0.5239	0.3042	0.2141	0.7434	0.5023	0.8404	0.2558	0.2552	0.5070	0.5802	0.4470	0.7735	0.5514	0.5772
XN	0.1047	0.2006	0.2150	0.1495	0.0637	0.2036	0.1333	0.2028	0.5833	0.1350	0.1376	0.2960	0.2419	0.2052	0.1492	0.3491
YC	0.2637	0.5214	0.7169	0.4460	0.1886	0.6068	0.4174	0.7600	0.3328	0.3945	0.4050	0.8860	0.7464	0.7041	0.4653	0.4736
ZZ	0.4195	0.7765	0.6338	0.7065	0.3038	0.7422	0.6568	0.7115	0.2171	0.6364	0.6554	0.5890	0.7067	0.7481	0.7202	0.2064
							SZ	SJZ	TY	TJ	UQ	WH	XA	XN	YC	ZZ
BJ	—	—	—	—	—	—	—	—	—	—	—	—	—	—	—	—
CC	—	—	—	—	—	—	—	—	—	—	—	—	—	—	—	—
CS	—	—	—	—	—	—	—	—	—	—	—	—	—	—	—	—
CD	—	—	—	—	—	—	—	—	—	—	—	—	—	—	—	—

(Continued)

Table 1. (Continued).

	BJ	CC	CS	CD	CQ	FZ	GZ	GY	HK	HZ	HB	HF	HT	JN	KM	LZ
CQ	-	-	-	-	-	-	-	-	-	-	-	-	-	-	-	-
FZ	-	-	-	-	-	-	-	-	-	-	-	-	-	-	-	-
GZ	-	-	-	-	-	-	-	-	-	-	-	-	-	-	-	-
GY	-	-	-	-	-	-	-	-	-	-	-	-	-	-	-	-
HK	-	-	-	-	-	-	-	-	-	-	-	-	-	-	-	-
HZ	-	-	-	-	-	-	-	-	-	-	-	-	-	-	-	-
HB	-	-	-	-	-	-	-	-	-	-	-	-	-	-	-	-
HF	-	-	-	-	-	-	-	-	-	-	-	-	-	-	-	-
HT	-	-	-	-	-	-	-	-	-	-	-	-	-	-	-	-
JN	-	-	-	-	-	-	-	-	-	-	-	-	-	-	-	-
KM	-	-	-	-	-	-	-	-	-	-	-	-	-	-	-	-
LZ	-	-	-	-	-	-	-	-	-	-	-	-	-	-	-	-
LS	1.0000	-	-	-	-	-	-	-	-	-	-	-	-	-	-	-
NC	0.2340	1.0000	-	-	-	-	-	-	-	-	-	-	-	-	-	-
NJ	0.1288	0.4574	1.0000	-	-	-	-	-	-	-	-	-	-	-	-	-
NN	0.1390	0.4937	0.7109	-	-	-	-	-	-	-	-	-	-	-	-	-
SH	0.0709	0.2280	0.3283	1.0000	-	-	-	-	-	-	-	-	-	-	-	-
SY	0.1071	0.3864	0.6812	0.6239	1.0000	-	-	-	-	-	-	-	-	-	-	-
SZ	0.0369	0.0478	0.4278	0.4529	0.2141	1.0000	-	-	-	-	-	-	-	-	-	-
SLZ	0.1165	0.4171	0.5808	0.6908	0.5117	0.8211	1.0000	-	-	-	-	-	-	-	-	-
TY	0.0789	0.2564	0.2002	0.2161	0.2624	0.4462	0.3009	1.0000	1.0000	-	-	-	-	-	-	-
TJ	0.0674	0.2215	0.3953	0.3794	0.9293	0.4951	0.2072	0.4971	0.1168	1.0000	-	-	-	-	-	-
UQ	0.2230	0.3262	0.4207	0.4541	0.2026	0.3368	0.3437	0.1603	0.4249	0.2123	1.0000	-	-	-	-	-
WH	0.1375	0.3287	0.8001	0.7743	0.4295	0.8119	0.4244	0.7428	0.2063	0.4164	0.3956	1.0000	-	-	-	-
XA	0.1099	0.3521	0.7226	0.7727	0.3798	0.6363	0.5111	0.6379	0.6227	0.3673	0.4511	0.7107	1.0000	-	-	-
YN	0.1657	0.1900	0.2027	0.2156	0.1025	0.1725	0.1645	0.1754	0.3313	0.1163	0.3359	0.1988	0.2229	1.0000	-	-
YC	0.1971	0.7000	0.6155	0.6605	0.3014	0.5290	0.6147	0.5269	0.3482	0.2989	0.6125	0.5994	0.7081	0.3056	1.0000	-
ZZ	0.1368	0.4533	0.6586	0.7764	0.4857	0.8156	0.4125	0.8545	0.5149	0.4728	0.3890	0.9207	0.7044	0.1921	0.5993	1.0000

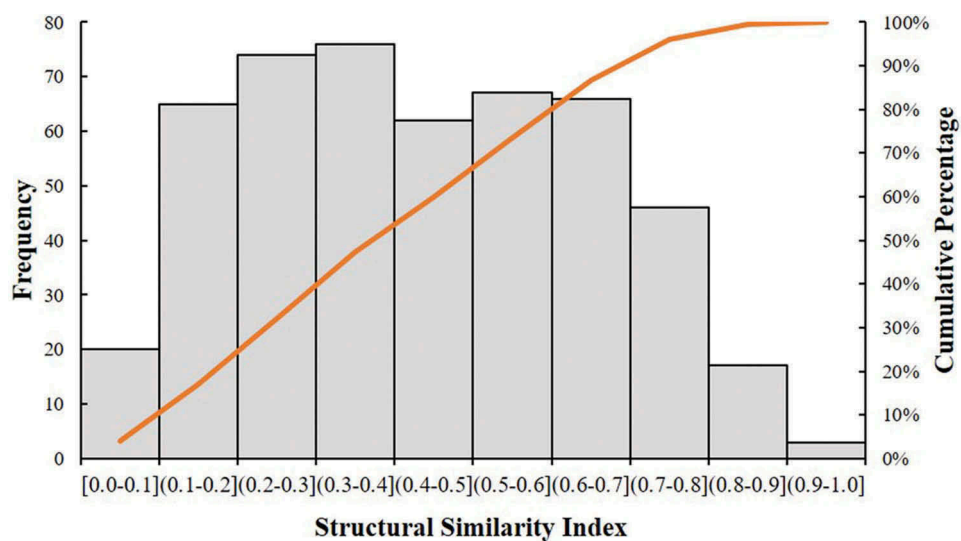


Figure 7. Histogram and cumulative frequency curve of the overall structural similarity indices.

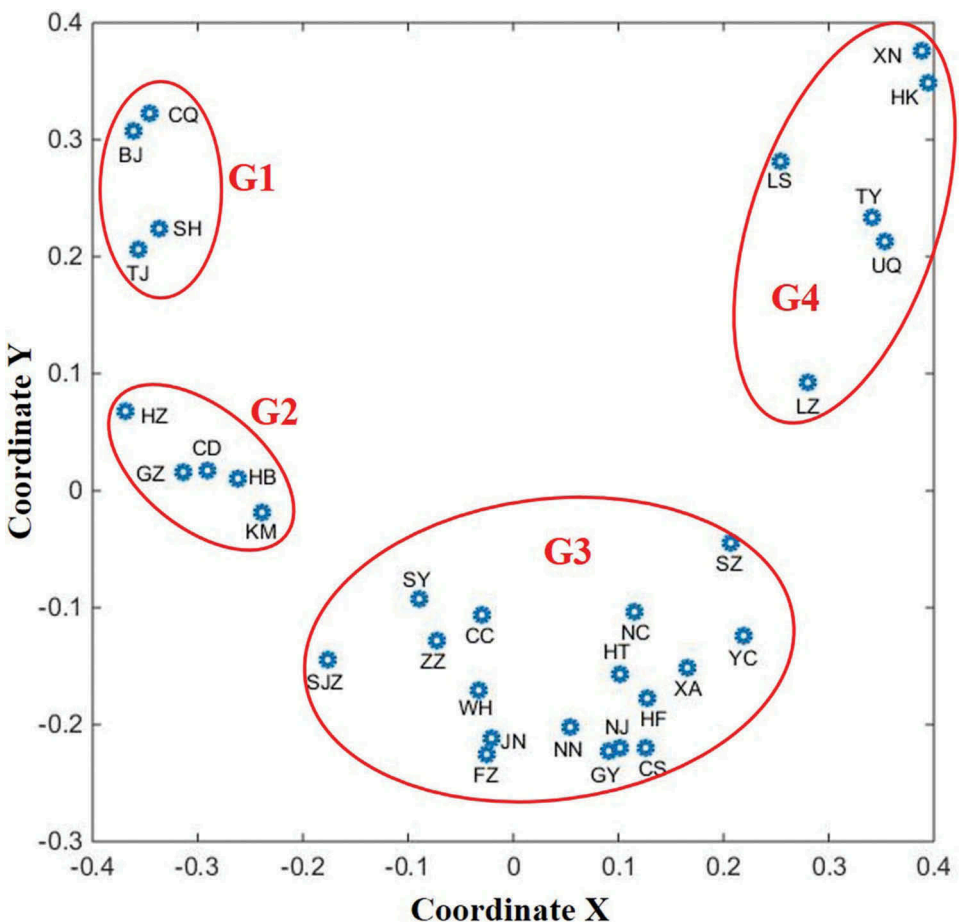


Figure 8. The multidimensional scaling for the 32 major cities in China.

including Guangzhou, Chengdu, Harbin, Kunming and Hangzhou. The third group (G3), displayed at the bottom of the MDS map, contains 17 cities, Shenzhen, Nanjing, Wuhan, Shenyang, Xi'an, Zhengzhou, Changchun, Changsha, Jinan, Shijiazhuang, Nanchang, Hefei, Nanning, Guiyang, Fuzhou, Hohhot and Yinchuan. On the upper-right of the MDS map, Taiyuan, Urumqi, Lanzhou, Xining, Haikou and Lhasa form the fourth group (G4). A summary statistics of the four groups is provided in Table 2. In combination with Figures 5 and 6, common features of the surface networks for the cities located in different groups can be identified. The cities in group G1 have not only the largest number of peaks, but also relatively high structural similarity indices between any two of them, while the cities in group G4 have the smallest number of peaks and relatively small structural similarity indices between any two of them.

Validation of extracted urban hierarchies

Facing China's rapid urbanization process, the Chinese government published a new standard for city-size classification in 2014, according to which each city is assigned to one of the five categories shown in Table 3.

To validate the urban classification obtained from NTL data, it was compared with the one according to the new Chinese standard. In Table 4 one can find the GDP data (China Statistical China Statistical Yearbook 2015) together with the urban population (China Urban Construction Statistical China Urban Construction Statistical Yearbook 2015) and

Table 2. The urban classification obtained from the night time light data.

Group	Cities	Peaks
G1	SH, BJ, CQ,TJ	Max = 563 Min = 337 Average = 424
G2	GZ, CD, HB, KM, HZ	Max = 301 Min = 255 Average = 270
G3	SZ, NJ, WH, SY, XA, ZZ, CC, CS, JN, SJZ, NC, HF, NN, GY, FZ, HT, YC	Max = 243 Min = 111 Average = 170
G4	TY, UQ, LZ, XN, HK, LS	Max = 123 Min = 57 Average = 90

Table 3. The five categories of cities classification.

Categories	Subcategories	Urban Population (million)
Super City	Super City	≥ 10
Megacity	Megacity	≥ 5 and < 10
Big City	Type I	≥ 3 and < 5
	Type II	≥ 1 and < 3
Medium City	Medium City	≥ 0.5 and < 1
Small City	Type I	≥ 0.2 and < 0.5
	Type II	< 0.2

Table 4. The referenced urban hierarchies based on the new standard.

City	Rank	GDP (billion RMB)	Urban Population (10,000 persons)	Area (1000 km ²)	Urban Hierarchy
SH	1	2530.00	2415.27	6.34	Super City
BJ	2	2300.00	1877.70	16.41	Super City
SZ	3	1750.00	1137.89	1.99	Super City
CQ	4	1610.00	1032.63	82.40	Super City
TJ	5	1720.00	676.84	11.94	Megacity
GZ	6	1810.00	615.10	7.43	Megacity
NJ	7	960.00	581.61	6.59	Megacity
CD	8	1080.00	494.41	14.31	Big City (Type I)
WH	9	1100.00	474.22	8.49	Big City (Type I)
SY	10	728.00	467.45	12.95	Big City (Type I)
XA	11	600.00	423.14	10.11	Big City (Type I)
HB	12	575.00	406.71	53.10	Big City (Type I)
ZZ	13	745.00	382.28	7.45	Big City (Type I)
KM	14	405.00	379.00	21.47	Big City (Type I)
CC	15	565.00	340.52	20.57	Big City (Type I)
CS	16	860.00	339.67	11.81	Big City (Type I)
HZ	17	1010.00	332.09	16.59	Big City (Type I)
TY	18	275.30	307.95	6.99	Big City (Type I)
JN	19	628.00	300.00	8.18	Big City (Type I)
SJZ	20	562.00	262.86	15.85	Big City (Type II)
UQ	21	273.00	261.70	14.22	Big City (Type II)
NC	22	400.00	241.84	7.40	Big City (Type II)
HF	23	560.00	209.79	11.44	Big City (Type II)
NN	24	341.00	208.45	22.11	Big City (Type II)
GY	25	269.20	196.10	8.03	Big City (Type II)
FZ	26	567.00	191.58	11.97	Big City (Type II)
LZ	27	200.00	186.58	13.09	Big City (Type II)
HT	28	309.10	132.00	17.22	Big City (Type II)
XN	29	113.10	120.63	7.68	Big City (Type II)
YC	30	148.00	108.91	9.49	Big City (Type II)
HK	31	116.10	108.00	3.15	Big City (Type II)
LS	32	38.90	27.00	31.66	Small City (Type I)

the area. A comparison of the city-size hierarchy given in Table 4 with the results shown in Figure 8 and Table 2, reveals a very good correspondence.

It is obvious that the urban classification given in Table 2 reflects the hierarchy due to the 2014 Chinese city size classification. To be more precise, all of the cities located in group G1 have a very high GDP and population density and are classified as *Super Cities* or *Megacities*.

All the cities located in group G2 belong to *Big cities, Type I*, with the exception of Guangzhou, which is situated at the heart of the most populous built-up metropolitan area in central-south China and classified as a *Megacity*. From Figure 6, the areas associated with high human activities' intensity are mostly distributed in the south-central of the city. Compared with the megacities in group G1, Guangzhou has less urban cores than the others.

For the 17 cities in group G3, all of them belong to *Big cities, Type I* or *Type II*, except Shenzhen and Nanjing. According to Table 4, Shenzhen is a super city, while Nanjing is a megacity. Compared with those super cities and megacities in group G1, Shenzhen has a smaller area and fewer critical points and lines in its surface network. Shenzhen was established as China's first special economic zone and was one of the fastest-growing cities in the world during the past 30 years. In the process of fast development, most of the super cities and megacities in group G1 have developed a dispersed expansion of

suburbanization, while Shenzhen has developed a dense central urban structure. Therefore, Shenzhen has less urban cores compared to other megacities.

All the cities in group G4 are *Big cities, Type II*, except Lhasa. In [Figure 8](#), Lhasa, which has the smallest number of critical points and critical lines in its surface networks, is placed far away from the other cities in the group. Overall, it can be said that the results obtained have a high consistency with the reference data, thus providing useful information for a better understanding of the urban system in China.

For comparison, the method proposed by Wu *et al.* (2014) was implemented in this study. Their approach measured, in a first step, the interaction intensity among different cities by using a gravity model based on night time light data. In a second step, a cluster analysis was performed to analyze the hierarchical structure of the urban system. As a result, three types of cities, viz., *national node cities*, *regional node cities* and *provincial node cities*, forming the urban hierarchies were determined. The seven national node cities included BJ, TJ, SH, GZ, HB, SY and CQ, the 22 regional node cities comprised CD, KM, HZ, SZ, NJ, WH, XA, ZZ, CC, CS, JN, SJZ, NC, HF, NN, GY, FZ, HT, YC, LZ, TY and LS, while only three cities, including UQ, XN and HK, were classified as provincial node cities. Evidently, most of the national node cities belong to groups G1 and G2, while the 22 regional node cities mainly concentrate in group G3 and the three provincial node cities in group G4. Summarizing, it can be said that both methods a similar classification of the urban hierarchy in mainland China is obtained. Compared with the new Chinese standard, the result extracted in this study shows a higher consistency and finer urban classification.

Discussion

In this paper, a method for characterizing urban hierarchies using NTL data was proposed, which has many potential applications in urban and regional studies, such as the determination of the size of cities, their spatial layouts or their organizational structures. The critical features of the surface networks extracted from NTL surfaces are directly related to urban elements, such as urban centers or transport hubs. In addition, the matrix of structural similarity indices can be used to classify cities according to their spatial forms, an important step with respect to the discussion on regional development strategies and the ongoing urban competitions (Giffinger and Gudrun 2010).

There are some limitations to the proposed approach. First, the extracted urban hierarchies are partly affected by administrative boundaries, which means that urban systems may vary in dependence of scale (Fang *et al.* 2017). Second, as cities vary in size and shape, the resulting surface networks are different, which may have additional impacts on the calculation of the structural similarity indices. Third, because in the present study the inter-city links were not taken into account, the resulting structural similarity indices were largely determined by the chosen threshold w . To be precise, a large threshold will generate large similarity indices, while a small threshold will result in small ones. As a general guideline, appropriate thresholds may be chosen by using a trial-and-error in combination with expert knowledge.

Conclusion

Urban hierarchies are closely related to economic growth, sustainable urban development and urban agglomeration. Examining urban hierarchies can help to shed light

on urban and regional development policies. Most previous studies used territory size, economic indicators, population and other statistical data as typical variables to determine urban size and growth. Due to the limited availability of reliable statistical data at fine scales, most previous studies failed to capture the detailed urban spatial information. Many studies have proved that night time light data have a significant correlation with many urban indicators and thus can be used to examine urban hierarchies. By detecting the structural similarity between surface networks from night time light distributions, the urban spatial structure at the city scale can be revealed. The structural similarity among cities is not only a measure for evaluating the level of cities' development, but also the reflection of urban development phases. Studying the structural similarity of urban spatial forms is helpful for understanding the similarities and differences in regional characteristics of different cities in urban and regional studies.

This study attempted to propose a novel method for examining urban hierarchies by measuring the structural similarity of night time light data. Surface networks are first constructed to extract the urban structures from the corresponding night time light surfaces, characterize them topologically by their associated night time light intensity graphs and quantify structural similarities between the cities by computing the maximum common induced subgraph. The approach allows the identification and visualization of the structural and morphological characteristics of night time light distribution. The novel method was applied to characterize the urban hierarchy among the 32 major cities of China. The results obtained were not only consistent with reference statistical data, but provided additional information about urban spatial structures.

In urban and regional studies, it is important to develop a method for measuring similarity or dissimilarity among the activity surfaces, such as population surfaces and human activity surfaces. In particular, researchers are interested in 'quantitative' or structural similarity rather than 'qualitative' similarity (Okabe and Masuyama 2006). Although the application in this paper is specific, the proposed methodological framework is so general that it may be applied to various urban studies, referring to urban functions and organizational structures. Further insights on the reason why the cities are structurally similar or dissimilar can be investigated by examining the relationship between the distribution of night time light intensity and the distribution of other urban features, such as population distribution, land cover and land use. Furthermore, the method is very flexible, thus inducing that it can be applied to various urban applications, such as the analysis of night time light dynamics or the detection of the dynamic patterns of urban agglomerations.

Acknowledgments

We are grateful to Prof. May Yuan and the three anonymous referees for their valuable comments and suggestions.

Disclosure statement

No potential conflict of interest was reported by the authors.

Funding

This work was supported by the National Key R&D Program of China [No. YS2017YFGH000441]; the National Natural Science Foundation of China [No. 41701462, 41801343, and 41871331]; the Major Program of National Social Science Foundation of China [No. 17ZDA068]; The China Postdoctoral Science Foundation [No. 2018M641960 and 2018M641961]; and the Fundamental Research Funds for the Central Universities of China.

Notes on contributors

Bin Wu is a postdoc researcher at the East China Normal University, China. He obtained his PhD in computer science in 2018 from the same university. His fields of interests are urban remote sensing, LiDAR, and spatio-temporal analysis.

Bailang Yu received the B.S. and Ph.D. degrees in cartography and geographic information systems from East China Normal University, Shanghai, China, in 2002 and 2009, respectively. He is currently a Professor with the Key Laboratory of Geographic Information Science, Ministry of Education, East China Normal University, Shanghai, where he is also with the School of Geographic Sciences. His research interests include urban remote sensing, nighttime light remote sensing, LiDAR, and object-based methods.

Shenjun Yao is an Associate Professor at East China Normal University. Her research interests focus on how the geographical information science and technology can be applied to the transportation and public health, as well as application of social sensing geodata.

Qiusheng Wu is an Assistant Professor in the Department of Geography at Binghamton University, State University of New York. His research interests focus on Geographic Information Science (GIS), remote sensing, and environmental modeling.

Zuoqi Chen received the PhD degree from East China Normal University, Shanghai, China, in 2017. Currently, he is a postdoctoral fellow with the Key Laboratories of Geographic Information Science (Ministry of Education) and School of Geographic Sciences, East China Normal University, Shanghai, China. His interested research fields contain urban remote sensing, nighttime light remote sensing, and development of GIS.

Jianping Wu received the M.S. degree from Peking University, Beijing, China, in 1986, and the Ph. D. degree from East China Normal University, Shanghai, China, in 1996. He is currently a Professor with East China Normal University. His research interests include remote sensing and geographic information system.

ORCID

Bailang Yu  <http://orcid.org/0000-0001-5628-0003>

Qiusheng Wu  <http://orcid.org/0000-0001-5437-4073>

References

- Batty, M., Longley, P., and Fotheringham, S., 1989. Urban growth and form: scaling, fractal geometry, and diffusion-limited aggregation. *Environment and Planning A*, 21 (11), 1447–1472. doi:10.1068/a211447
- Beaverstock, J.V., Smith, R.G., and Taylor, P.J., 1999. A roster of world cities. *Cities*, 16 (6), 445–458. doi:10.1016/S0264-2751(99)00042-6

- Bettencourt, L.M.A., 2013. The origins of scaling in cities. *Science*, 340 (6139), 1438–1441. doi:[10.1126/science.1235823](https://doi.org/10.1126/science.1235823)
- Borchert, J.R., 1967. American metropolitan evolution. *Geographical Review*, 57 (3), 301–332. doi:[10.2307/212637](https://doi.org/10.2307/212637)
- Bretagnolle, A., et al., 2009. The organization of urban systems. In: D. Lane, ed. *Complexity perspectives in innovation and social change*. Dordrecht, Netherlands: Springer, 197–220. doi:[10.1007/978-1-4020-9663-1_7](https://doi.org/10.1007/978-1-4020-9663-1_7)
- Chen, A.C.-L., et al., 2015. Approximating the maximum common subgraph isomorphism problem with a weighted graph. *Knowledge-Based Systems*, 85, 265–276. doi:[10.1016/j.knosys.2015.05.012](https://doi.org/10.1016/j.knosys.2015.05.012)
- Chen, X., 1991. China's city hierarchy, urban policy and spatial development in the 1980s. *Urban Studies*, 28 (3), 341–367. doi:[10.1080/00420989120080391](https://doi.org/10.1080/00420989120080391)
- Chen, Y. and Wang, J., 2014. Recursive subdivision of urban space and Zipf's law. *Physica A: Statistical Mechanics and Its Applications*, 395, 392–404. doi:[10.1016/j.physa.2013.10.022](https://doi.org/10.1016/j.physa.2013.10.022)
- Chen, Z., et al., 2017. A new approach for detecting urban centers and their spatial structure with night time light remote sensing. *IEEE Transactions on Geoscience and Remote Sensing*, 55 (11), 6305–6319. doi:[10.1109/TGRS.2017.2725917](https://doi.org/10.1109/TGRS.2017.2725917)
- China Statistical Yearbook, 2015. *China statistical yearbook*. Beijing: China Statistics Press.
- China Urban Construction Statistical Yearbook, 2015. *China urban construction statistical yearbook*. Beijing: China Statistics Press.
- Christaller, W., 1933. *Die zentralen Orte in Süddeutschland - Eine ökonomisch-geographische Untersuchung über die Gesetzmäßigkeit der Verbreitung und Entwicklung der Siedlungen mit städtischen Funktionen*. Jena: Fischer Verlag.
- Eeckhout, J., 2004. Gibrat's law for (all) cities. *The American Economic Review*, 94 (5), 1429–1451. doi:[10.1257/0002828043052303](https://doi.org/10.1257/0002828043052303)
- Elvidge, C.D., et al., 1997. Relation between satellite observed visible-near infrared emissions, population, economic activity and electric power consumption. *International Journal of Remote Sensing*, 18 (6), 1373–1379. doi:[10.1080/014311697218485](https://doi.org/10.1080/014311697218485)
- Fang, C., Pang, B., and Liu, H., 2017. Global city size hierarchy: spatial patterns, regional features, and implications for China. *Habitat International*, 66, 149–162. doi:[10.1016/j.habitatint.2017.06.002](https://doi.org/10.1016/j.habitatint.2017.06.002)
- Fang, C. and Yu, D., 2017. Urban agglomeration: an evolving concept of an emerging phenomenon. *Landscape and Urban Planning*, 162, 126–136. doi:[10.1016/j.landurbplan.2017.02.014](https://doi.org/10.1016/j.landurbplan.2017.02.014)
- Fang, J., et al., 2001. Changes in forest biomass carbon storage in China between 1949 and 1998. *Science*, 292 (5525), 2320–2322. doi:[10.1126/science.1058629](https://doi.org/10.1126/science.1058629)
- Giffinger, R. and Gudrun, H., 2010. Smart cities ranking: an effective instrument for the positioning of the cities? *ACE: Architecture, City and Environment*, 4 (12), 7–26. doi:[10.5821/ace.v4i12.2483](https://doi.org/10.5821/ace.v4i12.2483)
- Guerrero, D. and Proulhac, L., 2014. Freight flows and urban hierarchy. *Research in Transportation Business & Management*, 11, 105–115. doi:[10.1016/j.rtbm.2013.12.001](https://doi.org/10.1016/j.rtbm.2013.12.001)
- Joao, F.B., et al., 2014. The relationship between population dynamics and urban hierarchy: evidence from Portugal. *International Regional Science Review*, 37 (2), 149–171. doi:[10.1177/0160017614524226](https://doi.org/10.1177/0160017614524226)
- Li, X., et al., 2015. Detecting 2014 Northern Iraq insurgency using night-time light imagery. *International Journal of Remote Sensing*, 36 (13), 3446–3458. doi:[10.1080/01431161.2015.1059968](https://doi.org/10.1080/01431161.2015.1059968)
- Li, X. and Li, D., 2014. Can night-time light images play a role in evaluating the Syrian Crisis? *International Journal of Remote Sensing*, 35 (18), 6648–6661. doi:[10.1080/01431161.2014.971469](https://doi.org/10.1080/01431161.2014.971469)
- Liu, Z., et al., 2012. Extracting the dynamics of urban expansion in China using DMSP-OLS night time light data from 1992 to 2008. *Landscape and Urban Planning*, 106 (1), 62–72. doi:[10.1016/j.landurbplan.2012.02.013](https://doi.org/10.1016/j.landurbplan.2012.02.013)
- Lorenzen, M. and Andersen, K.V., 2009. Centrality and creativity: does Richard Florida's creative class offer new insights into urban hierarchy? *Economic Geography*, 85 (4), 363–390. doi:[10.1111/j.1944-8287.2009.01044.x](https://doi.org/10.1111/j.1944-8287.2009.01044.x)
- Maliszewski, P.J. and Huallacháin, B.Ó., 2012. Hierarchy and concentration in the American urban system of technological advance. *Papers in Regional Science*, 91 (4), 743–758. doi:[10.1111/j.1435-5957.2012.00422.x](https://doi.org/10.1111/j.1435-5957.2012.00422.x)

- Masuda, S., 2009. Qualitative analysis of two-dimensional urban employee distributions in Japan: a comparative study with urban population distributions by means of graph theoretic surface analysis. In: Y. Asami, Y. Sadahiro, and T. Ishikawa, eds. *New frontiers in urban analysis: in honor of Atsuyuki Okabe*. Boca Raton, FL: CRC Press, 115–131. doi:[10.1111/j.1538-4632.1984.tb00818.x](https://doi.org/10.1111/j.1538-4632.1984.tb00818.x)
- Mellander, C., et al., 2015. Night-Time light data: a good proxy measure for economic activity? *PLoS one*, 10 (10), e0139779. doi:[10.1371/journal.pone.0139779](https://doi.org/10.1371/journal.pone.0139779)
- Mu, L. and Wang, X., 2006. Population landscape: a geometric approach to studying spatial patterns of the US urban hierarchy. *International Journal of Geographical Information Science*, 20 (6), 649–667. doi:[10.1080/13658810600661342](https://doi.org/10.1080/13658810600661342)
- Neal, Z.P., 2011. From central places to network bases: a transition in the U.S. urban hierarchy, 1900–2000. *City & Community*, 10 (1), 49–75. doi:[10.1111/j.1540-6040.2010.01340.x](https://doi.org/10.1111/j.1540-6040.2010.01340.x)
- Newman, M.E., 2005. Power laws, Pareto distributions and Zipf's law. *Contemporary Physics*, 46 (5), 323–351. doi:[10.1080/00107510500052444](https://doi.org/10.1080/00107510500052444)
- Okabe, A. and Masuda, S., 1984. Qualitative analysis of two-dimensional urban population distributions in Japan. *Geographical Analysis*, 16 (4), 301–312. doi:[10.1111/j.1538-4632.1984.tb00818.x](https://doi.org/10.1111/j.1538-4632.1984.tb00818.x)
- Okabe, A. and Masuyama, A., 2006. A method for measuring structural similarity among activity surfaces and its application to the analysis of urban population surfaces in Japan. In: S. Rana, ed. *Topological data structures for surfaces: an introduction to geographical information science*. London, England: John Wiley & Sons, Ltd, 103–120. doi:[10.1002/0470020288.ch7](https://doi.org/10.1002/0470020288.ch7)
- Partridge, M.D., et al., 2008. Lost in space: population growth in the American hinterlands and small cities. *Journal of Economic Geography*, 8 (6), 727–757. doi:[10.1093/jeg/lbn038](https://doi.org/10.1093/jeg/lbn038)
- Partridge, M.D., et al., 2009. Agglomeration spillovers and wage and housing cost gradients across the urban hierarchy. *Journal of International Economics*, 78 (1), 126–140. doi:[10.1016/j.jinteco.2009.02.004](https://doi.org/10.1016/j.jinteco.2009.02.004)
- Pfaltz, J.L., 1976. Surface networks. *Geographical Analysis*, 8 (1), 77–93. doi:[10.1111/j.1538-4632.1976.tb00530.x](https://doi.org/10.1111/j.1538-4632.1976.tb00530.x)
- Pumain, D., 2006. Alternative explanations of hierarchical differentiation in urban systems. In: D. Pumain, ed. *Hierarchy in natural and social sciences*. Dordrecht: Netherlands: Springer, 169–222. doi:[10.1007/1-4020-4127-6_8](https://doi.org/10.1007/1-4020-4127-6_8)
- Raymond, J.W., Gardiner, E.J., and Willett, P., 2002. RASCAL: calculation of graph similarity using maximum common edge subgraphs. *The Computer Journal*, 45 (6), 631–644. doi:[10.1093/comjnl/45.6.631](https://doi.org/10.1093/comjnl/45.6.631)
- Raymond, J.W. and Willett, P., 2002. Maximum common subgraph isomorphism algorithms for the matching of chemical structures. *Journal of Computer-Aided Molecular Design*, 16 (7), 521–533. doi:[10.1023/a:1021271615909](https://doi.org/10.1023/a:1021271615909)
- Rosen, K.T. and Resnick, M., 1980. The size distribution of cities: an examination of the Pareto law and primacy. *Journal of Urban Economics*, 8 (2), 165–186. doi:[10.1016/0094-1190\(80\)90043-1](https://doi.org/10.1016/0094-1190(80)90043-1)
- Sadahiro, Y., 2001. Analysis of surface changes using primitive events. *International Journal of Geographical Information Science*, 15 (6), 523–538. doi:[10.1080/13658810110060433](https://doi.org/10.1080/13658810110060433)
- Shi, K., et al., 2014. Evaluating the ability of NPP-VIIRS night time light data to estimate the gross domestic product and the electric power consumption of China at multiple scales: a comparison with DMSP-OLS data. *Remote Sensing*, 6 (2), 1705–1724. doi:[10.3390/rs6021705](https://doi.org/10.3390/rs6021705)
- Shi, K., et al., 2015. Modelling and mapping total freight traffic in China using NPP-VIIRS night time light composite data. *GIScience & Remote Sensing*, 52 (3), 274–289. doi:[10.1080/15481603.2015.1022420](https://doi.org/10.1080/15481603.2015.1022420)
- Shi, K., et al., 2016a. Modeling spatiotemporal CO₂ (carbon dioxide) emission dynamics in China from DMSP-OLS night time stable light data using panel data analysis. *Applied Energy*, 168, 523–533. doi:[10.1016/j.apenergy.2015.11.055](https://doi.org/10.1016/j.apenergy.2015.11.055)
- Shi, K., et al., 2016b. Detecting spatiotemporal dynamics of global electric power consumption using DMSP-OLS night time stable light data. *Applied Energy*, 184, 450–463. doi:[10.1016/j.apenergy.2016.10.032](https://doi.org/10.1016/j.apenergy.2016.10.032)
- Small, C., et al. 2013. Mapping urban structure and spatial connectivity with VIIRS and OLS night light imagery. In: P. Gamba, ed. *Joint urban remote sensing event*. Sao Paulo, Brazil: IEEE, 230–233.

- Small, C., Pozzi, F., and Elvidge, C.D., 2005. Spatial analysis of global urban extent from DMSP-OLS night lights. *Remote Sensing of Environment*, 96 (3–4), 277–291. doi:[10.1016/j.rse.2005.02.002](https://doi.org/10.1016/j.rse.2005.02.002)
- Taafe, E.J., 1962. The urban hierarchy: an air passenger definition. *Economic Geography*, 38 (1), 1–14. doi:[10.2307/142321](https://doi.org/10.2307/142321)
- Takahashi, S., et al., 1995. Algorithms for extracting correct critical points and constructing topological graphs from discrete geographical elevation data. *Computer Graphics Forum*, 14 (3), 181–192. doi:[10.1111/j.1467-8659.1995.cgf143_0181.x](https://doi.org/10.1111/j.1467-8659.1995.cgf143_0181.x)
- Tsogo, L., Masson, M.H., and Bardot, A., 2000. Multidimensional scaling methods for many-object sets: a review. *Multivariate Behavioral Research*, 35 (3), 307–319. doi:[10.1207/S15327906MBR3503_02](https://doi.org/10.1207/S15327906MBR3503_02)
- Welch, R., 1980. Monitoring urban population and energy utilization patterns from satellite data. *Remote Sensing of Environment*, 9 (1), 1–9. doi:[10.1016/0034-4257\(80\)90043-7](https://doi.org/10.1016/0034-4257(80)90043-7)
- Wolf, G.W., 1991. A FORTRAN subroutine for cartographic generalization. *Computers & Geosciences*, 17 (10), 1359–1381. doi:[10.1016/0098-3004\(91\)90002-U](https://doi.org/10.1016/0098-3004(91)90002-U)
- Wolf, G.W., 2004. Topographic surfaces and surface networks. In: S. Rana, ed. *Topological data structures for surfaces*. London, England: John Wiley & Sons Ltd, 15–30. doi:[10.1002/0470020288.ch2](https://doi.org/10.1002/0470020288.ch2)
- Wolf, G.W., 2014. Knowledge diffusion from GIScience to other fields: the example of the usage of weighted surface networks in nanotechnology. *International Journal of Geographical Information Science*, 28 (7), 1401–1424. doi:[10.1080/13658816.2014.889298](https://doi.org/10.1080/13658816.2014.889298)
- Wolf, G.W., 2017. Scale independent surface characterisation: geography meets precision surface metrology. *Precision Engineering*, 49, 456–480. doi:[10.1016/j.precisioneng.2016.12.005](https://doi.org/10.1016/j.precisioneng.2016.12.005)
- Wu, B., et al., 2017. A graph-based approach for 3D building model reconstruction from airborne LiDAR point clouds. *Remote Sensing*, 9 (1), 92. doi:[10.3390/rs9010092](https://doi.org/10.3390/rs9010092)
- Wu, B., et al., 2018. An extended minimum spanning tree method for characterizing local urban patterns. *International Journal of Geographical Information Science*, 32 (3), 450–475. doi:[10.1080/13658816.2017.1384830](https://doi.org/10.1080/13658816.2017.1384830)
- Wu, J., et al., 2014. Hierarchical structure and spatial pattern of China's urban system: evidence from DMSP/OLS nightlight data. *Acta Geographica Sinica*, 69 (6), 759–770. doi:[10.11821/dlxb201406004](https://doi.org/10.11821/dlxb201406004)
- Wu, Q., et al., 2015. A localized contour tree method for deriving geometric and topological properties of complex surface depressions based on high-resolution topographical data. *International Journal of Geographical Information Science*, 29 (12), 2041–2060. doi:[10.1080/13658816.2015.1038719](https://doi.org/10.1080/13658816.2015.1038719)
- Xue, J., 2008. Hierarchical structure and distribution pattern of Chinese urban system based on aviation network. *Geographical Research*, (01), 23–32+242. doi:[10.11821/yj2008010003](https://doi.org/10.11821/yj2008010003)
- Yu, B., et al., 2014. Object-based spatial cluster analysis of urban landscape pattern using night time light satellite images: a case study of China. *International Journal of Geographical Information Science*, 28 (11), 2328–2355. doi:[10.1080/13658816.2014.922186](https://doi.org/10.1080/13658816.2014.922186)
- Yu, B., et al., 2015. Poverty evaluation using NPP-VIIRS night time light composite data at the county level in China. *IEEE Journal of Selected Topics in Applied Earth Observations and Remote Sensing*, 8 (3), 1217–1229. doi:[10.1109/JSTARS.2015.2399416](https://doi.org/10.1109/JSTARS.2015.2399416)
- Zhang, C., et al., 2015. Research on city system spatial structure of the Yangtze river economic belt: based on DMSP/OLS night time light data. *Urban Development Studies*, 22 (3), 19–27. doi:[10.3969/j.issn.1006-3862.2015.03.003](https://doi.org/10.3969/j.issn.1006-3862.2015.03.003)
- Zhong, C., et al., 2017. Revealing centrality in the spatial structure of cities from human activity patterns. *Urban Studies*, 54 (2), 437–455. doi:[10.1177/0042098015601599](https://doi.org/10.1177/0042098015601599)
- Zhong, Y. and Lu, Y., 2011. Hierarchical structure and distribution pattern of Chinese urban system based on railway network. *Geographical Research*, 30 (5), 785–794. doi:[10.11821/yj2008010003](https://doi.org/10.11821/yj2008010003)